Paternal Low Protein Diet Programs Preimplantation Embryo Gene Expression, Fetal Growth and Skeletal Development in Mice

Adam J. Watkins[a], Slobodan Sirovica[b], Ben Stokes[c], Mark Isaacs[d], Owen Addison[e], Richard A. Martin[b]

[a] Aston Research Centre for Healthy Ageing, School of Life and Health Sciences, Aston University, Birmingham, B4 7ET, United Kingdom.

[b] School of Engineering and Applied Science and Aston Research Centre for Healthy Ageing, Aston University, Birmingham, B4 7ET, United Kingdom.

[c] School of Life and Health Sciences, Aston University, Birmingham, B4 7ET, United Kingdom.

[d] European Bioenergy Research Institute, Aston University, Birmingham B4 7ET, United Kingdom.

[e] Biomaterials Unit, University of Birmingham School of Dentistry, College of Medical and Dental Sciences, Edgbaston, Birmingham, B15 2TT, United Kingdom

Corresponding Author:

Adam J. Watkins: Aston Research Centre for Healthy Ageing, School of Life and Health Sciences, Aston University, Birmingham, B4 7ET, United Kingdom. E mail: a.watkins1@aston.ac.uk

Abstract

Defining the mechanisms underlying the programming of early life growth is fundamental for improving adult health and wellbeing. While the association between maternal diet, offspring growth and adult disease risk is well-established, the effect of father's diet on offspring development are largely unknown. Therefore, we fed male mice an imbalanced low protein diet (LPD) to determine the impact on post-fertilisation development and fetal growth. We observed that in preimplantation embryos derived from LPD fed males, expression of multiple genes within the central metabolic AMPK pathway was reduced. In late gestation, paternal LPD programmed increased fetal weight, however, placental weight was reduced, resulting in an elevated fetal:placental weight ratio. Analysis of gene expression patterns revealed increased levels of transporters for calcium, amino acids and glucose within LPD placentas. Furthermore, placental expression of the epigenetic regulators *Dnmt1* and *Dnmt3L* were increased also, coinciding with altered patterns of maternal and paternal imprinted genes. More strikingly, we observed fetal skeletal development was perturbed in response to paternal LPD. Here, while offspring of LPD fed males possessed larger skeletons, their bones comprised lower volumes of high mineral density in combination with reduced maturity of bone apatite. These data offer new insight in the underlying programming mechanisms linking poor paternal diet at the time of conception with the development and growth of his offspring.

Keywords: Blastocyst metabolism; Bone health; Developmental programming; Fetal growth; Paternal diet; Placental function.

Abbreviations

AMPK	5' AMP-activated protein kinase
DOHaD	Developmental Origins of Health and Disease
E	Embryonic day
FWHM	Full width at half maximum
LPD	Low protein diet
mTORC1	mechanistic Target of Rapamycin complex 1
NPD	Normal protein diet
SXRD	Synchrotron x-ray diffraction
µ-CT	micro-computed tomography

1. Introduction

It is estimated that up to 60% of global mortality is attributed to non-communicable diseases such as type 2 diabetes, obesity and heart disease [1]. Typically, the risk for developing such disorders is associated with adult lifestyle factors including poor diet, lack of exercise and smoking. However, strong associations between maternal nutrition, fetal growth, weight at birth and an increased risk for adult-onset ill-health have been identified [2, 3]. The Developmental Origins of Health and Disease (DOHaD) hypothesis identifies perturbed early life growth and nutrition as critical factors in determining adult risk for cardiovascular and metabolic disease. In addition, links between growth during prenatal and postnatal development and degenerative disorders such as osteoporosis have also been identified [2]. Central to elucidating the biological mechanisms underlying the programming of long-term ill-health has been the use of animal models. For example, modification of maternal diet or metabolic status in rodents exclusively during the preimplantation period of development has been shown to impact negatively on blastocyst metabolism and redox status [4-7], resulting in persistent changes in offspring growth, adult metabolic homeostasis and cardiovascular function [8-10]. Studies have identified that during sub-optimal environmental conditions, the preimplantation embryo initiates cellular and physiological mechanisms intended to support maximal post-implantation development and survival [4, 10, 11]. However, the long-term consequences of these embryonic adaptive responses can increase cardio-metabolic and bone health disease risk in later life. Such studies reveal the dynamic interaction between the embryo and the immediate environment, as well as the long-term impacts for offspring health.

Post-implantation, the development and function of the placenta is central in the regulation of fetal growth. Changes in placental function may result in differential transfer of essential nutrients between maternal and fetal systems, programming altered fetal growth. We have shown that in response to maternal low protein diet (LPD, 9% protein) fed exclusively during the preimplantation period, early post-implantation trophoblast outgrowths display increased spreading and cell division phenotypes

[4, 12]. Studies feeding pregnant mice [13] and rats [14] a LPD identify changes in placental mechanistic Target of Rapamycin complex 1 (mTORC1) and amino acid transporter protein expression, as well as perturbed gene expression for apoptosis, growth inhibition and DNA methylation processes. In addition, changes in placental structure, nutrient uptake and transport have also been reported in response to maternal diet [15-18]. These studies indicate that appropriate placental development and function plays a pivotal role in directing fetal growth, an essential indicator of postnatal offspring phenotype and disease risk.

While the consequences of manipulating the maternal environment have received extensive investigation, the impact of paternal nutrition on the development and growth of his offspring remains poorly defined. However, there is now a growing body of clinical, epidemiological and animal model data highlighting new associations between paternal physiological status and offspring health [19]. Studies in humans and mice have demonstrated that elevated paternal BMI impacts negatively on sperm quantity, quality, DNA integrity and male reproductive fitness [20-23]. Post-fertilisation, poor paternal diet disrupts blastocyst metabolism [24], skeletal formation [25], neonatal hepatic lipid and cholesterol biosynthesis, IGF-1 and corticosterone levels [26, 27], pancreatic β-cell function [28] and adiposity [29]. Using the well-characterised rodent LPD model, we demonstrated previously that offspring from LPD fed male mice were heavier at birth, displayed elevated adult adiposity, glucose intolerance, cardiovascular dysfunction and elevated serum TNF-α when compared to offspring from normal protein diet (NPD; 18% protein) fed males [30].

As enhanced perinatal growth is a significant risk factor for adult health status, the aim of our current study was to define the mechanisms linking paternal diet with offspring development and growth. Here, we report that paternal LPD decreases blastocyst expression of multiple metabolic AMPK pathway genes, enhances fetal growth and elevates placental expression of central nutrient

transporters and fetal growth regulating imprinted genes. In addition, we observe changes in fetal skeletal development and bone mineral deposition patterns.

2. Materials and methods

2.1 Animal Treatments

All experimental procedures were conducted using protocols approved by, and in accordance with, the UK Home Office Animal (Scientific Procedures) Act 1986 and local ethics committee at Aston University. Male (8 week old) and female (8 week old) C57BL/6 mice (Charles River, Oxford, UK) were maintained at Aston University Biomedical Facility on a 07:00–19:00 light-dark cycle, temperature of 20–22°C with *ad libitum* access to chow (Special Dietary Services Ltd, UK) and water. Male mice were housed singly and allocated either control normal protein diet (NPD; 18 % casein; 180 g / kg diet; n = 8) or isocaloric low protein diet (LPD; 9% casein; 90 g / kg diet; n = 8) (Special Dietary Services Ltd, UK; Supplementary Table 1; protein content confirmed by manufacturer) for between 7 and 9 weeks in total to ensure all stages of spermatogenesis and spermiogenesis were exposed to the diets [31]. We have reported previously on the physiological impact of LPD on paternal physiology [30], demonstrating no impairment in paternal fertility (sperm number, pregnancy rate, litter size), serum glucose, insulin or testosterone levels or in testicular weight when compared with NPD fed males. Virgin 8-9 week old C57BL/6 females were caged singly overnight with either NPD or LPD studs. Plug positive females were housed singly and maintained on chow *ad libitum* for either collection of blastocysts at E3.5, or late gestation fetal tissues at E17.

Blastocysts were flushed from the oviducts and uterus at E3.5 using EmbryoMax KSOM medium (Millipore; Catalogue number MR-020P-5F), washed and pooled into groups of 25, frozen in volumes <10µl and stored at -80^{o}C ahead of PCR array analysis. At E17, dams were culled via cervical dislocation for the collection of fetal and extra-embryonic tissues as described previously [12].

Briefly, individual concepti were dissected from the uterine tissue and weighed prior to separation and weighing individually of the fetus, placenta and yolk sac. Fetal heart and liver tissues were isolated, weighed, snap frozen in liquid nitrogen and stored. Isolated placentae were either snap frozen or fixed in 10% formalin (Sigma, UK) for 24 hours at 4^{o}C prior to storage in 70% ethanol at 4^{o}C. In addition, whole fetuses were fixed in 10% formalin (Sigma, UK) for 24 hours at 4^{o}C prior to storage in 70% ethanol at 4^{o}C ahead of skeletal analyses.

2.2 Blastocyst AMPK RT^2 PCR array

Total RNA was isolated from eight individual pools of 25 blastocysts (four NPD and four LPD; each pool obtained from 4-5 females) using the RNeasy Plus Micro kit (Qiagen, UK) according to the manufacturer's instructions. RNA concentration was assessed using the Qubit fluorometer (Thermo Scientific, UK) and equivalent quantities of RNA were converted to cDNA using the RT^2 First Strand cDNA synthesis kit (Qiagen, UK) according to the manufacturer's instructions. Expression of 84 AMPK signalling pathway genes (S1 Table online) were analysed using the AMPK signalling PCR array (Qiagen, UK). Amplification was performed on a Stratagene Mx 3000P System (Agilent Technologies, CA. USA) with resultant gene expression analysed using web-based PCR Array Data Analysis software (www.SAbiosciences.com).

2.3 Tissue metabolite measurement, RNA extraction and transcript expression.

Flushed day 3.5 maternal uteri were homogenised (50 mM HEPES, 150 mM NaCl, 1 mM EDTA, 1 mM EGTA, 1% SDS) prior to protein level determination (DC assay, Bio-Rad Laboratories) and glucose level analysis by glucose oxidase assay (Sigma, UK) in accordance with the manufacturer's instructions, and measured on a Benchmark microplate reader (Bio-Rad Laboratories, UK).

RNA was isolated from placental and fetal liver using the RNeasy Mini Kit (Qiagen, UK) with additional on-column DNase I digestion (Qiagen, UK), prior to cDNA synthesis (nanoScript 2 reverse

transcription kit; Primerdesign, UK), all according to manufacturer's instructions. For Real-Time PCR (qRT-PCR), 5 ng cDNA was added to a mastermix comprising 10 µl 2X mastermix (Precision SYBRgreen Mastermix; Primerdesign, UK), 5 µM forward and reverse primers and 8.3 µl water per reaction. Amplification and detection was performed using a Stratagene Mx 3000P System (Agilent Technologies, USA). The expression levels of the samples were calculated using the $\Delta\Delta C_T$ method with placental data normalised to the expression of *Sdha* and *Tbp* and liver tissue data normalised to *Pgk1* and *Tbp* [32, 33]. Reaction specificity was confirmed by dissociation curve analysis. Primer sequences are provided in Supplementary Table 3.

2.4 Determination of fetal sex and placental histology

DNA was extracted from fetal tail tissue using the DNeasy Blood and Tissue kit (Qiagen, UK) according to the manufacturer's instruction. For PCR determination of fetal sex, 2 µl (100 ng) of template DNA was added to a mastermix comprising 12.5 µl mastermix (2X JumpStart Taq; Sigma), 2.5 ul primer mix (25 µM forward and reverse primers) and 8 µl water per reaction. Amplification was performed using an Eppendorf (Mastercycler® Pro) thermocycler using primers specific for regions on the Y (*Sry*) and X (Dxnds3) chromosomes (primer sequences are provided in Supplementary Table 3).

Formalin fixed placentas from five male and five female fetuses per diet group (only one male and female taken from any individual dam, n = 5 dams per diet group) were embedded in paraffin wax. From each placenta, 4 midsagittal 5 µm sections were taken from the midline of the placenta. Sections were mounted onto slides ahead of haematoxylin and eosin staining. Sections were imaged using a CETI Magnum-T microscope and a Jenoptik ProgRes CF camera prior to determination of total junctional and labyrinthine zone areas using Volocity software. Areas were expressed as proportion (percentage) of total midsagittal area comprised by junctional and labyrinthine zones.

2.5 Fetal bone analyses

2.5.1 Whole fetal µ-CT analysis

Whole formalin fixed fetuses were scanned using a Skyscan 1172 *in vivo* µ-CT scanner (Bruker, Belgium). All scans were taken at 50 kVa and 170 µA with a 0.5 mm aluminium filter, 700 ms exposure time, 180^{o} tomographic rotation. Individual two-dimensional cross-sectional images were reconstructed using Bruker NRecon software (version 1.6.10) and were analysed using Bruker CTAn software (version 1.15). Voxel resolution was 13.5 µm. After 3D reconstruction of each fetal mouse, bony tissues were determined by a global threshold that was set using a combination of visual inspection of the 2D images and the analysis of associated histograms. Bony tissue was identified in all individual fetuses. A threshold for bony tissue was set at 700 Hounsfield Units following visual confirmation in all samples. Using this threshold, a clear distinction between bone, surrounding soft tissue and ringing artefacts (inconclusive signals near sharp transitions) could be made.

2.5.2 Synchrotron x-ray diffraction (SXRD)

The right femur and humerus from formalin fixed NPD and LPD fetuses were dissected clean of surrounding muscle and connective tissue and stored in 70% ethanol at 4^{o}C. SXRD measurements of NPD and LPD offspring fetal femur and humerus bones were conducted at beamline B16 Diamond Light Source (Oxford Harwell Campus, Didcot, UK). Bones were mounted normal to the impinging X-rays in transmission geometry to allow measurements in two orthogonal directions perpendicular to the X-ray beam. An incident X-ray energy of 17 keV was used, equivalent to a wavelength (λ) of 0.7293 Å, with a beam size of 35 µm. For each sample, three separate line transects separated by 1 mm above and below the midline of the bone were scanned in 25 µm increments and an exposure time of 60 seconds. Diffraction data was collected using a 2D area detector (Image Star 9000, Photonic Science Ltd. UK) with a 3056 x 3056 pixel resolution, placed 110 mm behind the sample to give a 2θ range of 5-33°. Measurements were taken also for the direct beam, empty sample

containers, beryllium windows and water, with all measurements and instrument parameters determined against silicon and lanthanum hexaboride (LaB_6) standards.

2.5.3 SXRD data analysis

Diffraction data were normalised and background corrected using the Fit2D software package (version 12.077, ESRF). Diffraction patterns were azimuthally integrated to produce 1D spectra of intensity (*I*) versus the scattering angle (2θ). The Bragg peak corresponding to the (002) (~13°) reflection was fitted with a Gaussian peak shape to obtain the peak position and the full width at half maximum (FWHM) to quantify possible changes to the crystal structure from the lattice parameters. Additionally, Rietveld refinement was used to determine changes in the lattice parameters and texture coefficients (General Structure Analysis System package). A hexagonal unit cell with a $P6_3/m$ symmetry space group was assumed for the hydroxyapatite structural model with initial lattice parameters [34]. The positions of the (002) and (300) planes were used calculate the hydroxyapatite unit cell *c* and *a* axis lattice parameters. Peak positions were used to determine the inter-planar spacing (*d*), where $d = \lambda/2sin\,\theta$ (here θ is equivalent to half the angle between the incident X-rays and the detector), from which lattice parameters were calculated. A hexagonal unit cell was assumed for hydroxyapatite, where the relationship between the *d* spacing, Miller indices for a given Bragg peak and lattice parameters are given as;

$$\frac{1}{d^2} = \frac{4}{3}\left(\frac{h^2 + hk + k^2}{a^2}\right) + \frac{l^2}{c^2}$$

2.5.4 Fetal femur Inductive Coupled Plasma (ICP) elemental analysis

Isolated formalin-fixed fetal right femurs were digested (1 ml concentrated nitric acid, 20 mg of ammonium fluoride) using in a CEM SP-D discover microwave digester (190^{o}C for 20 minutes, 300W power). Samples were diluted with 4 ml of deionised water prior to ICP analysis for calcium and phosphorus content using an iCAP 7000 ICP-OES system and measured against AAS standards

for calcium and phosphorus (Sigma, UK). The R-squared of the calcium and phosphorus calibration curves were 0.9991 and 0.9993 respectively.

2.6 Statistical analyses

Data were assessed for normality (Shapiro–Wilk test) and correlations between phenotypic measurements (Pearson correlation) using SPSS (Version 21). Analysis of fetal weights, bone development and placental morphology were analysed using a multilevel random effects regression model (SPSS version 21), adjusting for paternal duration on respective diet (number of days), paternal origin of litter, gestational litter size and body weight effects where appropriate [10]. Where a significant effect of sex was observed, data for each sex were analysed separately and reported as such. Significance was taken at $P<0.05$.

3. Results

3.1 Paternal LPD reduces blastocyst AMPK signalling pathways gene expression

Virgin 8-week old female C57BL6 mice were mated with either NPD or LPD fed male C57BL6 mice for the collection of mid-late stage (E3.5) blastocysts. We observed no significant difference in the mean number of blastocysts collected from NPD or LPD mated females (NPD = 8.6 ± 0.2, LPD = 8.4 ± 0.4; P = 0.84). Four pools of 25 mid-late blastocysts were collected for each paternal dietary group ahead of AMPK pathway PCR array analysis. In total, 71 genes were decreased in their relative expression and 18 genes were increased in LPD blastocysts (Fig. 1A) (see Supplementary Table 2 for array gene list, fold expression differences and individual P values). There was no significant difference in the expression of any of the reference genes (*Actb, B2m, Gapdh, Gusb, Hsp90ab1*) between groups ($P < 0.1$). In LPD blastocysts, 16 genes were identified as being significantly decreased in their expression, relative to NPD blastocysts ($P < 0.05$), while no genes displayed a significant increase in expression. Gene function analysis of the differentially expressed genes characterised them into the following biological processes: metabolism (*Cpt1b, Slc2a4*) (Fig. 1B),

receptors (*Adra1b, Adra2b, Adipor1*) (Fig. 1C), transcription regulation (*Crtc2, Foxo3, Trp53*) (Fig. 1D), signalling cascades (*Akt2, Pdpk1, Prkab1, Ppp2r4*) (Fig. 1E) and protein synthesis and autophagy (*Eef2k, Rb1cc1, Stradb, Ulk1*) (Fig. 1F). Analysis of flushed maternal uterine tissue revealed significantly lower glucose levels in females mated with LPD fed males; NPD = 2.27 ± 0.21, LPD = 1.15 ± 0.28 µg/ml/mg uterus (P = 0.007).

3.2 Fetal growth and placental development are altered by paternal LPD

As fetal growth is reflective of weight at birth, postnatal growth and adult disease risk, we investigated whether paternal LPD influenced late gestation (E17) fetal development. At the time of cull, paternal LPD had no effect on mean litter size (NPD = 8, LPD = 8; P = 0.52) or maternal weight gain (NPD = 9.3 ± 0.4g, LPD 8.9 ± 0.5g; P = 0.59). In addition, there was no effect of the number of days individual males were fed LPD on fetal weight (P = 0.59), placental weight (P = 0.71) or on fetal:placental weight ratio (P = 0.66). In LPD offspring, we observed a similar weight of the conceptus (combined fetal, placental and yolk sac weight; P = 0.06) but elevated weight of the isolated fetus (P = 0.012), while placental weight was decreased significantly (P = 0.011) (Fig. 2A). There was no difference in mean yolk sac weight between groups (Fig. 2A). While fetal heart weight was not different between NPD and LPD offspring (data not shown), fetal liver weight was increased significantly in LPD offspring (NPD = 42.7 ± 1.0 mg, LPD = 47.0 ± 0.9 mg; P = 0.005). Analysis of organ:body weight ratios revealed a significantly decreased fetal:placenta weight ratio (P< 0.0001), but no difference in fetal:liver or fetal:heart ratios (Fig. 2B). To determine whether changes in AMPK metabolic signalling established within the preimplantation embryo persisted into fetal tissues, we determined the expression of 6 genes in the fetal liver differentially expressed from our blastocyst array. We chose to study genes involved in a broad range of cellular processes to ascertain the potential scope of differences being maintained into late gestation fetal tissues. Here, the expression of *Adipor1, Akt2, Prkaca, Ppargc1a* and *Trp53* were all reduced significantly in LPD livers (Fig. 2C; P < 0.05), mirroring LPD embryonic expression profiles.

3.3 Paternal LPD alters placental morphology and gene expression

Placental development and function are central regulators of fetal growth. Therefore, we assessed the placental morphology and gene expression patterns in response to paternal diet. NPD and LPD placentas displayed equivalent mean mid-line placental cross sectional area (Fig. 3B), with no differences in mean labyrinth zone, junctional zone or trophoblast areas (Fig. 3B). However, when assessed as relative proportions of the whole placental area, a significant reduction in labyrinth and increase in junctional zones were observed in LPD placentas ($P = 0.028$ and 0.002 respectively; Fig. 3C). As an increased fetal:placental ratio indicates net flux of nutrients to the fetus per gram placenta is upregulated, we assessed placental expression of key nutrient transporters. Here, expression of the calcium (*Atp2b1),* neutral amino acid (*Slc38a2)* and glucose (*Slc2a1, Slc2a4)* transporters were increased significantly in LPD placentas (Fig. 3D, $P < 0.05$). No difference in the expression of the parathyroid hormone receptor (*Pthr1*) or vitamin D3 receptor (*Vdr)* were observed between groups. In addition, increased expression of DNA methyltransferase 1 and 3L (*Dnmt1, Dnmt3L*) (Fig. 3E), and differential expression of the maternally imprinted *Cdkn1c, H19,* and *Grb10* and paternally imprinted *Mest* and *Snrpn* genes were observed in LPD placentas (Fig. 3F; all $P < 0.05$).

3.4 Paternal LPD modifies fetal skeletal development and bone crystallographic morphology

To determine whether the enhanced fetal growth observed in LPD offspring was driven by changes in skeletal formation, we assessed whole fetal skeletal morphology using micro computed tomography (μ-CT) (Fig. 4A). Despite there being no difference in whole skeletal bone mineral density (Fig. 4B), LPD offspring displayed a significantly increased mean skeletal volume (Fig. 4C, $P = 0.037$). As a consequence of the increased LPD skeletal volume, mean total litter mineral content was elevated by 47% (Fig. 4D, $P = 0.037$). Analysis of whole skeletal mineral distribution, revealed an increase in total area of mineralised bone (Fig. 4E), reflective of the increase in bone volume in LPD offspring. However, LPD skeletons displayed significantly increased proportions of low mineral

density bone (700-1290 Hounsfield units, Fig. 4F, G, $P < 0.0001$) but decreased proportions of high mineral density bone (1300-1900 Hounsfield units, Fig. 4F, H; $P < 0.01$).

To quantify further the impact of paternal diet on offspring bones, we analysed fetal femur and humerus hydroxyapatite crystalline structure by X-ray diffraction (Fig. 5B). As no difference in hydroxyapatite crystalline structure was observed between humerus and femur bones (data not shown), data from each bone were combined and are presented as an average. We observed differences in the scattering angle spectra with significant broadening in the LPD bones (Fig. 5C). Analysis of a=b lattice (16^{o} scattering angle) and c lattice (13^{o} scattering angle) parameters revealed increases in the mean lattice parameters for LPD offspring (Fig. 5D, F; $P <0.001$) with concordant increases in mean lattice full width half maximum values (Fig. 5E, G; $P < 0.001$). Analysis of the a/c lattice ratio revealed similar mean values of 0.707 and 0.709 for NPD and LPD bones respectively. To determine whether the changes in hydroxyapatite lattice parameters were as a result of changes in bone mineral composition, we performed Inductive Coupled Plasma (ICP) elemental analysis on individual fetal femurs. We observed no difference in bone calcium or phosphorus content, or in their ratio (Table 1).

4. Discussion

Defining the mechanisms underlying the aetiology of adult-onset disorders such as obesity, heart disease and osteoporosis are of considerable relevance to current human health concerns. Strong associations between maternal diet, altered embryonic and fetal development and increased adult-onset disease risk in her offspring are well established. However, our understanding of the impact paternal diet has on post-fertilisation development and adult offspring health remains ill-defined. Previously, we demonstrated that a nutritionally imbalanced paternal LPD in mice elevated offspring growth, increased adult fat mass, impaired glucose tolerance and cardiovascular function [30]. As increased perinatal growth is a significant risk factor for adult health, the aim of this current study

was to define the impact of paternal diet on post-fertilisation development and fetal growth regulation. In response to paternal LPD, we observed persistent programming of multiple AMPK genes, established within the preimplantation embryos and still evident in the late gestation fetal liver. In addition, we observed enhanced fetal growth, coinciding with elevated expression of placental nutrient transporters and imprinted genes. Finally, we observed that while offspring of LPD males had increased skeleton volume, their bones comprised higher volumes of low mineral density.

Paternal LPD reduced blastocyst expression of 16 genes within the central cellular metabolic AMPK pathway. We observed decreased expression of genes for receptors, signalling cascades, protein synthesis and autophagy, transcription regulation and metabolism biological processes. Of note, we observed reductions in the expression of the adiponectin receptor 1 (*Adipor1*), the facilitated glucose transporter 4 (*Slc2a4*) and the energy sensing non-catalytic subunit of AMPK (*Prkab1*), as well as insulin receptor (*Insr*; at a trend level). Together, these observations indicate a reduced metabolic status within LPD embryos. In response to a drop in intracellular ATP levels, AMPK stimulates the uptake of glucose and oxidation of fatty acids and inhibits the synthesis of cholesterol and triglycerides [35]. In mammalian preimplantation embryos, glucose is the predominant energy substrate with mouse embryos capable of additionally metabolising fatty acids [36]. In both mouse and human embryos, while glucose uptake correlates positively with embryonic development, blastocoel formation and post implantation survival [37, 38], lower glycolytic rates (the conversion of glucose to lactate) are observed in 'faster' developing mouse embryos [38]. Conversely, lower rates of amino acid and glucose metabolism in human embryos have been attributed to increased developmental potential [39]. Therefore, the reduced expression of *Slc2a4*, *Adipor1* and *Prkab1* observed in LPD blastocysts may be a direct adaptive response initiated to modify metabolism in order to enhance post-implantation survival.

In line with reduced signalling via metabolic receptors, we observed that paternal LPD reduced the expression of signal transduction regulators *Akt2* and *Pdpk1* in LPD blastocysts. Akt and Pdpk1 have key roles in the regulation of cellular migration, metabolism mitogenesis, differentiation and survival through their down-stream interaction with mTORC1 [40]. In response to growth factor receptor signalling, mTORC1 stimulates the biosynthesis of proteins, lipids and nucleic acids via the actions of the down-stream substrates ribosomal protein S6 kinase (S6K) and eukaryotic translation initiation factor 4E-binding protein (4E-BP) [41]. Changes in mouse blastocyst signalling via the mTORC1 pathway have been demonstrated in response to uterine amino acid and insulin concentrations [4]. Therefore, it cannot be discounted that changes in blastocyst metabolism and downstream signalling mechanisms may have occurred in response to paternal modulation of the maternal pre-implantation uterine environment. Indeed, we observed reductions in maternal uterine glucose levels at the time of implantation in females mated with LPD fed males. Changes in uterine metabolite levels have been observed in response to maternal LPD [4] associated with enhanced fetal growth and adult cardiovascular and metabolic ill-health in mice [9, 10]. Studies have also shown that seminal plasma can impact on rodent, porcine and human female reproductive tract physiology [42, 43]. The presence of seminal plasma at the time of mating is essential for the appropriate oviductal expression of several embryotrophic factors including *Lif, IL6, Csf* and *Egf* and the pro-apoptotic factor *Trail* in mice [44]. In line with these studies, we observed decreased expression of the transformation related protein 53 (*Trp53*) in LPD blastocysts. Trp53 acts as a tumour suppressor in many cell types either by reducing cell cycle progression or by induction of pro-apoptotic factors. While increased expression of Trp53 is associated with poor embryonic developmental capacity in both mice and humans [45, 46], *Trp53*$^{-/-}$ mouse blastocysts display increased viability post-transfer and are more likely to result in a viable fetus [47]. These data indicate that paternal diet may modify blastocyst metabolism and survival directly as well as via modulation of the maternal uterine environment. However, further mechanistic studies are required to determine the association of paternal diet with modified

preimplantation embryo metabolism and gene expression and their impact on subsequent developmental potential.

Our second key finding was that in late gestation, fetal growth was increased in response to paternal LPD while placental size was decreased. The mechanisms underlying the reduced size of the mature placenta in females mated with LPD fed males remain unclear. Maternal LPD fed exclusively during the preimplantation period modifies blastocyst allocation to the trophectoderm lineage with consequent changes in trophoblast out-growth phenotype [4, 12]. Therefore, reduced placental weight may be reflective of differential cell lineage allocation in the early embryo, driven either by uterine changes in specific nutrients and/or perturbed blastocyst metabolic signalling. The observation that despite a significant reduction in LPD placental mass, LPD offspring fetal weight was enhanced, suggests placental transport flux of nutrients to the fetus was upregulated. Therefore, we determined the expression levels of placental transporters central in the regulation of fetal growth. Paternal LPD resulted in an increased expression of specific transporters of glucose (*Slc2a1, Slc2a4*), neutral amino acids (*Slc38a2*) and calcium (*Atp2b1*). Elevated placental expression and activity of glucose and System A and L amino acid transporters are associated with increased fetal growth in women with type-1 diabetes [48, 49]. Similarly in obese women, increased amino acid transporter activities correlate positively with fetal growth [50], while placental size and calcium transporter gene expression have been shown to predict offspring bone mass at birth [51, 52]. Therefore, up-regulation of placental nutrient transporter expression appears a central mechanism in the regulation of fetal growth, whatever the underlying environmental cause. In contrast, the impact of paternal physiological status on placental development has remained largely unexplored. In a mouse model of paternal dietary-induced obesity, sex-specific changes in placental expression of *Ppara* and *Casp12* have been observed [53], while a paternal low folate diet modified placental expression of genes associated with gene transduction and cell signalling [25]. Thus, programming of enhanced placental nutrient transport may underlie the enhanced fetal growth trajectory induced by paternal LPD.

However, the conclusion drawn from our current study are limited by our observations being taken only at the gene expression level. It is essential that our future studies validate these changes at the protein level in order to determine fully the impact of paternal diet on fetal growth regulation and the underlying mechanisms involved. In addition, it would also be beneficial to measure placental function and nutrient transport flux in response to paternal diet.

The paternal epigenome also plays a substantial role in directing fetal growth through regulation of placental development and function [54]. In mammals, fetal growth and placental transport of nutrients are regulated tightly by the expression of parent-of-origin specific imprinted genes [55]. Imprinted genes have evolved to regulate maternal resource allocation to the developing fetus, with paternal imprints allocating resources to the fetus and maternal imprints retaining them. In LPD placentas we observed increased levels of the maternally-expressed *Cdkn1c, H19* and *Grb10,* while the paternally-expressed *Mest* and *Snrpn* were increased and decreased respectively. In addition, we observed increased *Dnmt1* and *Dnmt3L* expression in LPD placentas. *Cdkn1c* encodes a cyclin-dependent kinase inhibitor that negatively regulates cell proliferation [56]. Reduced placental expression of *Cdkn1c* is associated with increased placental size and disproportionate labyrinth/junctional zone proportions [56, 57]. Similarly, disruption of the maternal *Grb10* allele also results in overgrowth of both the placenta and the fetus via enhanced placental efficiency [58, 59]. The paternally expressed *Mest* is restricted to fetal endothelial cells of the labyrinth [60] with loss of function resulting in reduced placental size and fetal growth [61]. It was of interest to note that while we observed increased expression of *H19,* no difference in *Igf2* was detected. As *Igf2* and *H19* expression are regulated reciprocally from the same differentially methylated element, an increase in *H19* should result in a decrease in expression of *Igf2.* However, as we did not measurement parental allele-specific expression, or Igf2 at the protein level, this may account for the lack of difference observed. Similarly, we did not determine the impact of our observed changes in *Dnmt1/3L* expression on placental gene methylation status or expression profile. Our observations of decreased

placental size in conjunction with increased expression of maternal *Cdkn1c, H19* and *Grb10,* as well as decreased paternal *Snrpn,* indicate a maternal adaptive mechanisms to restrict fetal growth in response to paternal LPD. However, the increased placental expression of nutrient transporters may ultimately result in the elevated fetal growth observed. It is also possible that LPD induced changes in paternal gene expression may also influence placental function and offspring development independent of direct transmission of genetic effects [62, 63]. Therefore further studies are needed, not only to address our study limitations and validate the gene expression changes observed for regulators of epigenetic mechanisms, but also to understand the heritability and paternal genomic mechanisms of fetal programming.

Our third main finding was that paternal LPD modified the development of the fetal skeleton. While the skeletal volume of LPD fetuses was increased, we observed that their bones comprised lower levels of high density hydroxyapatite mineral deposition. Studies in humans and rodent models have shown that appropriate development of the fetal skeleton appears to be a fundamental prerequisite for optimal adult bone health. In humans, fetal femur longitudinal growth predicts skeletal size at age 4 years [64], and variation in older-adult bone mass is highly correlated with prenatal skeletal development and birth weight [65]. Human studies demonstrate also that nutritionally induced delays in bone maturation increase hip fracture risk, reduce bone mineral accrual and induce disproportionate bone growth in adulthood [66, 67]. In rodents, maternal LPD has been shown to reduce femoral neck thickness, trabecular density and femoral and tibia strength in adult offspring [68]. Conversely, a paternal low folate diet in mice results in an increase in fetal skeletal defects [25], while sperm DNA damage has been associated with embryonic malformations [69]. These data indicate that while paternal LPD promotes overall bone size and skeletal growth, their composition appears sub-optimal.

The changes in offspring bone mineral distribution were observed alongside significant crystallographic changes in bone apatite. We observed that in femurs and humerus bones of offspring

from LPD fed males, both a=b and c lattice parameters were increased significantly from those of NPD offspring. Such changes are usually ascribed to either compositional variation in the apatite crystallites [70, 71] or crystallographic differences relative to the crystallite particle morphology [72] manifested due to the presence of internal residual strains. We observed that the ratio of the unit cell parameters c/a remained similar between NPD and LPD diets at 0.707 and 0.709 respectively. These differences are therefore more likely to be related to growth-rate induced effects than phenomena associated with (later) bone maturation where typically the a-lattice decreases whilst the c-lattice remains constant [73]. Similarly, the lack of distortion of the unit-cell (lack of changes to the c/a ratio) suggests that in this case, differences in macroscopically manifested residual stresses in LPD and NPD bone are unlikely to account for the observed changes to the unit-cell as such stresses in bone are deviatoric. Within bone the chemical composition of hydroxyapatite varies. Although no quantitative phase analysis was undertaken it is well accepted that with bone growth and maturation, there is an increase in bone crystallinity, a matched crystallite growth and a reduction in lattice size [63]. Changes in the lattice parameters of early forming bone can inform on compositional differences of the maturing bone apatite. Studies have demonstrated that the substitution of apatite OH^- and PO_4 ions with Cl^- and HPO_4^{2-} respectively, significantly lengthens the a=b apatite axis [64], while the substitution of PO_4 by CO_3 increases the apatite c lattice axis [65]. In addition, changes in lattice parameters have been identified based on the analysis of calcium and phosphorus content during the early stages of ossification in animal [65, 66] and human [63] studies. Here, developing bone is seen as a mixture impure hydroxyapatite with calcium-phosphate phases comprising different calcium:phosphate ratios. As bones mature, the calcium content increases as a function of age. However, our elemental analysis of NPD and LPD fetal femurs revealed no significant difference in mean calcium or phosphorus content, or in their relative ratio. One main limitation to elemental analysis is that it cannot discriminate between calcium contained within a crystalline state and that within more amorphous states. Our data suggests that the more rapid skeletal growth associated with the LPD diet is associated with smaller crystallite sizes and increased unit-cell lengths which are in

contrast to the expected observation of an increased crystallite size with age/growth rate and a reduction of unit-cell lengths bone maturation [70]. These findings indicate undescribed perturbation of bone growth with disruption of 'normal' mineralization at the ultrastructural level. Although the exact physico-chemical mechanisms could not be elucidated there are clear implications on bone function and further studies to determine whether this is a delay in ossification or a more permanent disruption of ossification are required.

Conclusions

We have demonstrated that paternal LPD perturbs blastocyst metabolic AMPK gene expression, potentially as an adaptive mechanism to preserve embryo viability. Analysis of late gestation fetal liver tissues revealed identical expression profiles for several of the same genes indicating persistence in paternally programmed metabolic function between the embryo and late gestation differentiated tissues. Furthermore, we observed that paternal LPD enhanced fetal growth potentially through elevated expression of placental nutrient transporter and modified patterns of imprinted gene expression. Finally, we observed that while paternal LPD promoted increased fetal skeletal growth, bone mineral distribution was impaired. These studies highlight the importance of paternal nutrition at the time of conception for the post-fertilisation development and growth of his offspring. While these adaptive changes in developmental trajectory may confer short-term advantage, for example in post-implantation survival or post-natal reproductive fitness, they result ultimately in an increased predisposition for adult-onset chronic disease in later life. However, our current conclusions are limited in their scope and require additional studies to confirm whether our observed changes at the gene levels are reflected in changes at the protein levels. In addition, it is essential that we defining further the precise mechanisms underlying the programming of offspring development in relation to paternal diet.

Acknowledgements

The authors would like to thank the staff at Aston University's Biomedical Research Unit for animal provision and maintenance. The authors would also like to acknowledge the technical assistance provided by Michelle Holder for the analysis of fetal skeletal bone formation by μ-CT, Ian Pape at the Diamond Light source synchrotron facility and Professor Karen Wilson and the Surfaces, Materials and Catalysis group in the European Bioenergy Research Institute.

Funding

This work was supported by an Aston Research Centre for Healthy Ageing fellowship awarded to AJW, a Society for Reproduction and Fertility Academic scholarship awarded to AJW, and Diamond Light source synchrotron facility beam time awarded for B16 to AW, SS, OA and RAM.

Competing interests

The authors declare that there are no competing interests associated with this manuscript.

References

[1] Y.C. Wang, K. McPherson, T. Marsh, S.L. Gortmaker, M. Brown, Health and economic burden of the projected obesity trends in the USA and the UK, Lancet, 378 (2011) 815-825.

[2] M.A. Hanson, P.D. Gluckman, Early developmental conditioning of later health and disease: physiology or pathophysiology?, Physiological reviews, 94 (2014) 1027-1076.

[3] K.D. Sinclair, A.J. Watkins, Parental diet, pregnancy outcomes and offspring health: metabolic determinants in developing oocytes and embryos, Reproduction, fertility, and development, 26 (2013) 99-114.

[4] J.J. Eckert, R. Porter, A.J. Watkins, E. Burt, S. Brooks, H.J. Leese, P.G. Humpherson, I.T. Cameron, T.P. Fleming, Metabolic induction and early responses of mouse blastocyst developmental programming following maternal low protein diet affecting life-long health, PloS one, 7 (2012) e52791.

[5] N. Igosheva, A.Y. Abramov, L. Poston, J.J. Eckert, T.P. Fleming, M.R. Duchen, J. McConnell, Maternal diet-induced obesity alters mitochondrial activity and redox status in mouse oocytes and zygotes, PloS one, 5 (2010) e10074.

[6] R.G. Lea, J.E. McCracken, S.S. McIntyre, W. Smith, J.D. Baird, Disturbed development of the preimplantation embryo in the insulin-dependent diabetic BB/E rat, Diabetes, 45 (1996) 1463-1470.

[7] K.H. Moley, M.M. Chi, C.M. Knudson, S.J. Korsmeyer, M.M. Mueckler, Hyperglycemia induces apoptosis in pre-implantation embryos through cell death effector pathways, Nat Med, 4 (1998) 1421-1424.

[8] W.Y. Kwong, A.E. Wild, P. Roberts, A.C. Willis, T.P. Fleming, Maternal undernutrition during the preimplantation period of rat development causes blastocyst abnormalities and programming of postnatal hypertension, Development, 127 (2000) 4195-4202.

[9] A.J. Watkins, E.S. Lucas, A. Wilkins, F.R. Cagampang, T.P. Fleming, Maternal periconceptional and gestational low protein diet affects mouse offspring growth, cardiovascular and adipose phenotype at 1 year of age, PloS one, 6 (2011) e28745.

[10] A.J. Watkins, E. Ursell, R. Panton, T. Papenbrock, L. Hollis, C. Cunningham, A. Wilkins, V.H. Perry, B. Sheth, W.Y. Kwong, J.J. Eckert, A.E. Wild, M.A. Hanson, C. Osmond, T.P. Fleming, Adaptive responses by mouse early embryos to maternal diet protect fetal growth but predispose to adult onset disease, Biology of reproduction, 78 (2008) 299-306.

[11] C. Sun, M.A. Velazquez, S. Marfy-Smith, B. Sheth, A. Cox, D.A. Johnston, N. Smyth, T.P. Fleming, Mouse early extra-embryonic lineages activate compensatory endocytosis in response to poor maternal nutrition, Development, 141 (2014) 1140-1150.

[12] A.J. Watkins, E.S. Lucas, S. Marfy-Smith, N. Bates, S.J. Kimber, T.P. Fleming, Maternal nutrition modifies trophoblast giant cell phenotype and fetal growth in mice, Reproduction, 149 (2015) 563-575.

[13] C.P. Gheorghe, R. Goyal, J.D. Holweger, L.D. Longo, Placental gene expression responses to maternal protein restriction in the mouse, Placenta, 30 (2009) 411-417.

[14] F.J. Rosario, N. Jansson, Y. Kanai, P.D. Prasad, T.L. Powell, T. Jansson, Maternal protein restriction in the rat inhibits placental insulin, mTOR, and STAT3 signaling and down-regulates placental amino acid transporters, Endocrinology, 152 (2011) 1119-1129.

[15] J.A. Armitage, I.Y. Khan, P.D. Taylor, P.W. Nathanielsz, L. Poston, Developmental programming of the metabolic syndrome by maternal nutritional imbalance: how strong is the evidence from experimental models in mammals?, The Journal of physiology, 561 (2004) 355-377.

[16] P.M. Coan, O.R. Vaughan, J. McCarthy, C. Mactier, G.J. Burton, M. Constancia, A.L. Fowden, Dietary composition programmes placental phenotype in mice, The Journal of physiology, 589 (2011) 3659-3670.

[17] E. Kim, Mechanisms of amino acid sensing in mTOR signaling pathway, Nutrition research and practice, 3 (2009) 64-71.

[18] A.N. Sferruzzi-Perri, O.R. Vaughan, M. Haro, W.N. Cooper, B. Musial, M. Charalambous, D. Pestana, S. Ayyar, A.C. Ferguson-Smith, G.J. Burton, M. Constancia, A.L. Fowden, An obesogenic diet during mouse pregnancy modifies maternal nutrient partitioning and the fetal growth trajectory, FASEB journal : official publication of the Federation of American Societies for Experimental Biology, 27 (2013) 3928-3937.

[19] J. Li, O. Tsuprykov, X. Yang, B. Hocher, Paternal programming of offspring cardiometabolic diseases in later life, J Hypertens, 34 (2016) 2111-2126.

[20] J.E. Chavarro, J. Furtado, T.L. Toth, J. Ford, M. Keller, H. Campos, R. Hauser, Trans-fatty acid levels in sperm are associated with sperm concentration among men from an infertility clinic, Fertility and sterility, 95 (2011) 1794-1797.

[21] B.I. Ghanayem, R. Bai, G.E. Kissling, G. Travlos, U. Hoffler, Diet-induced obesity in male mice is associated with reduced fertility and potentiation of acrylamide-induced reproductive toxicity, Biology of reproduction, 82 (2010) 96-104.

[22] A.O. Hammoud, M. Gibson, J. Stanford, G. White, D.T. Carrell, M. Peterson, In vitro fertilization availability and utilization in the United States: a study of demographic, social, and economic factors, Fertility and sterility, 91 (2009) 1630-1635.

[23] H.I. Kort, J.B. Massey, C.W. Elsner, D. Mitchell-Leef, D.B. Shapiro, M.A. Witt, W.E. Roudebush, Impact of body mass index values on sperm quantity and quality, J Androl, 27 (2006) 450-452.

[24] N.K. Binder, M. Mitchell, D.K. Gardner, Parental diet-induced obesity leads to retarded early mouse embryo development and altered carbohydrate utilisation by the blastocyst, Reproduction, fertility, and development, 24 (2012) 804-812.

[25] R. Lambrot, C. Xu, S. Saint-Phar, G. Chountalos, T. Cohen, M. Paquet, M. Suderman, M. Hallett, S. Kimmins, Low paternal dietary folate alters the mouse sperm epigenome and is associated with negative pregnancy outcomes, Nature communications, 4 (2013) 2889.

[26] L.M. Anderson, L. Riffle, R. Wilson, G.S. Travlos, M.S. Lubomirski, W.G. Alvord, Preconceptional fasting of fathers alters serum glucose in offspring of mice, Nutrition, 22 (2006) 327-331.

[27] B.R. Carone, L. Fauquier, N. Habib, J.M. Shea, C.E. Hart, R. Li, C. Bock, C. Li, H. Gu, P.D. Zamore, A. Meissner, Z. Weng, H.A. Hofmann, N. Friedman, O.J. Rando, Paternally induced transgenerational environmental reprogramming of metabolic gene expression in mammals, Cell, 143 (2010) 1084-1096.

[28] S.F. Ng, R.C. Lin, D.R. Laybutt, R. Barres, J.A. Owens, M.J. Morris, Chronic high-fat diet in fathers programs beta-cell dysfunction in female rat offspring, Nature, 467 (2010) 963-966.

[29] N.O. McPherson, T. Fullston, W.X. Kang, L.Y. Sandeman, M.A. Corbett, J.A. Owens, M. Lane, Paternal under-nutrition programs metabolic syndrome in offspring which can be reversed by antioxidant/vitamin food fortification in fathers, Scientific reports, 6 (2016) 27010.

[30] A.J. Watkins, K.D. Sinclair, Paternal low protein diet affects adult offspring cardiovascular and metabolic function in mice, American journal of physiology. Heart and circulatory physiology, 306 (2014) H1444-1452.

[31] E.F. Oakberg, Duration of spermatogenesis in the mouse and timing of stages of the cycle of the seminiferous epithelium, The American journal of anatomy, 99 (1956) 507-516.

[32] E.S. Lucas, A.J. Watkins, A.L. Cox, S.J. Marfy-Smith, N. Smyth, T.P. Fleming, Tissue-specific selection of reference genes is required for expression studies in the mouse model of maternal protein undernutrition, Theriogenology, 76 (2011) 558-569.

[33] J. Vandesompele, K. De Preter, F. Pattyn, B. Poppe, N. Van Roy, A. De Paepe, F. Speleman, Accurate normalization of real-time quantitative RT-PCR data by geometric averaging of multiple internal control genes, Genome biology, 3 (2002) RESEARCH0034.

[34] Y. Meheust, K.D. Knudsen, J.O. Fossum, Inferring orientation distributions in anisotropic powders of nano-layered crystallites from a single two-dimensional WAXS image, J Appl Crystallogr, 39 (2006) 661-670.

[35] M.M. Mihaylova, R.J. Shaw, The AMPK signalling pathway coordinates cell growth, autophagy and metabolism, Nat Cell Biol, 13 (2011) 1016-1023.

[36] N. Hillman, T.J. Flynn, The metabolism of exogenous fatty acids by preimplantation mouse embryos developing in vitro, Journal of embryology and experimental morphology, 56 (1980) 157-168.

[37] D.K. Gardner, P.L. Wale, R. Collins, M. Lane, Glucose consumption of single post-compaction human embryos is predictive of embryo sex and live birth outcome, Human reproduction, 26 (2011) 1981-1986.

[38] Y.S. Lee, G.A. Thouas, D.K. Gardner, Developmental kinetics of cleavage stage mouse embryos are related to their subsequent carbohydrate and amino acid utilization at the blastocyst stage, Human reproduction, 30 (2015) 543-552.

[39] C.G. Baumann, D.G. Morris, J.M. Sreenan, H.J. Leese, The quiet embryo hypothesis: molecular characteristics favoring viability, Molecular reproduction and development, 74 (2007) 1345-1353.

[40] P. Castel, H. Ellis, R. Bago, E. Toska, P. Razavi, F.J. Carmona, S. Kannan, C.S. Verma, M. Dickler, S. Chandarlapaty, E. Brogi, D.R. Alessi, J. Baselga, M. Scaltriti, PDK1-SGK1 Signaling Sustains AKT-Independent mTORC1 Activation and Confers Resistance to PI3Kalpha Inhibition, Cancer cell, 30 (2016) 229-242.

[41] J.J. Howell, S.J. Ricoult, I. Ben-Sahra, B.D. Manning, A growing role for mTOR in promoting anabolic metabolism, Biochemical Society transactions, 41 (2013) 906-912.

[42] S.A. Robertson, Seminal plasma and male factor signalling in the female reproductive tract, Cell and tissue research, 322 (2005) 43-52.

[43] D.J. Sharkey, K.P. Tremellen, M.J. Jasper, K. Gemzell-Danielsson, S.A. Robertson, Seminal fluid induces leukocyte recruitment and cytokine and chemokine mRNA expression in the human cervix after coitus, Journal of immunology, 188 (2012) 2445-2454.

[44] J.J. Bromfield, J.E. Schjenken, P.Y. Chin, A.S. Care, M.J. Jasper, S.A. Robertson, Maternal tract factors contribute to paternal seminal fluid impact on metabolic phenotype in offspring, Proceedings of the National Academy of Sciences of the United States of America, 111 (2014) 2200-2205.

[45] X.L. Jin, V. Chandrakanthan, H.D. Morgan, C. O'Neill, Preimplantation embryo development in the mouse requires the latency of TRP53 expression, which is induced by a ligand-activated PI3 kinase/AKT/MDM2-mediated signaling pathway, Biology of reproduction, 81 (2009) 234-242.

[46] D. Wells, M.G. Bermudez, N. Steuerwald, H.E. Malter, A.R. Thornhill, J. Cohen, Association of abnormal morphology and altered gene expression in human preimplantation embryos, Fertility and sterility, 84 (2005) 343-355.

[47] A. Li, V. Chandrakanthan, O. Chami, C. O'Neill, Culture of zygotes increases TRP53 [corrected] expression in B6 mouse embryos, which reduces embryo viability, Biology of reproduction, 76 (2007) 362-367.

[48] T. Jansson, M. Wennergren, T.L. Powell, Placental glucose transport and GLUT 1 expression in insulin-dependent diabetes, American journal of obstetrics and gynecology, 180 (1999) 163-168.

[49] A.G. Kuruvilla, S.W. D'Souza, J.D. Glazier, D. Mahendran, M.J. Maresh, C.P. Sibley, Altered activity of the system A amino acid transporter in microvillous membrane vesicles from placentas of macrosomic babies born to diabetic women, The Journal of clinical investigation, 94 (1994) 689-695.

[50] N. Jansson, F.J. Rosario, F. Gaccioli, S. Lager, H.N. Jones, S. Roos, T. Jansson, T.L. Powell, Activation of placental mTOR signaling and amino acid transporters in obese women giving birth to large babies, The Journal of clinical endocrinology and metabolism, 98 (2013) 105-113.

[51] C.R. Holroyd, N.C. Harvey, S.R. Crozier, N.R. Winder, P.A. Mahon, G. Ntani, K.M. Godfrey, H.M. Inskip, C. Cooper, S.W.S.S. Group, Placental size at 19 weeks predicts offspring bone mass at birth: findings from the Southampton Women's Survey, Placenta, 33 (2012) 623-629.

[52] R. Martin, N.C. Harvey, S.R. Crozier, J.R. Poole, M.K. Javaid, E.M. Dennison, H.M. Inskip, M. Hanson, K.M. Godfrey, C. Cooper, R. Lewis, S.W.S.S. Group, Placental calcium transporter (PMCA3) gene expression predicts intrauterine bone mineral accrual, Bone, 40 (2007) 1203-1208.

[53] N.K. Binder, S.A. Beard, T.J. Kaitu'u-Lino, S. Tong, N.J. Hannan, D.K. Gardner, Paternal obesity in a rodent model affects placental gene expression in a sex-specific manner, Reproduction, 149 (2015) 435-444.

[54] S.J. Tunster, H.D. Creeth, R.M. John, The imprinted Phlda2 gene modulates a major endocrine compartment of the placenta to regulate placental demands for maternal resources, Developmental biology, 409 (2016) 251-260.

[55] P. Georgiades, A.C. Ferguson-Smith, G.J. Burton, Comparative developmental anatomy of the murine and human definitive placentae, Placenta, 23 (2002) 3-19.

[56] K. Takahashi, T. Kobayashi, N. Kanayama, p57(Kip2) regulates the proper development of labyrinthine and spongiotrophoblasts, Molecular human reproduction, 6 (2000) 1019-1025.

[57] S.J. Tunster, M. Van de Pette, R.M. John, Fetal overgrowth in the Cdkn1c mouse model of Beckwith-Wiedemann syndrome, Dis Model Mech, 4 (2011) 814-821.

[58] M. Charalambous, M. Cowley, F. Geoghegan, F.M. Smith, E.J. Radford, B.P. Marlow, C.F. Graham, L.D. Hurst, A. Ward, Maternally-inherited Grb10 reduces placental size and efficiency, Developmental biology, 337 (2010) 1-8.

[59] M. Charalambous, F.M. Smith, W.R. Bennett, T.E. Crew, F. Mackenzie, A. Ward, Disruption of the imprinted Grb10 gene leads to disproportionate overgrowth by an Igf2-independent mechanism, Proceedings of the National Academy of Sciences of the United States of America, 100 (2003) 8292-8297.

[60] W. Mayer, M. Hemberger, H.G. Frank, R. Grummer, E. Winterhager, P. Kaufmann, R. Fundele, Expression of the imprinted genes MEST/Mest in human and murine placenta suggests a role in angiogenesis, Developmental dynamics : an official publication of the American Association of Anatomists, 217 (2000) 1-10.

[61] L. Lefebvre, S. Viville, S.C. Barton, F. Ishino, E.B. Keverne, M.A. Surani, Abnormal maternal behaviour and growth retardation associated with loss of the imprinted gene Mest, Nat Genet, 20 (1998) 163-169.

[62] B. Hocher, H. Haumann, J. Rahnenfuhrer, C. Reichetzeder, P. Kalk, T. Pfab, O. Tsuprykov, S. Winter, U. Hofmann, J. Li, G.P. Puschel, F. Lang, D. Schuppan, M. Schwab, E. Schaeffeler, Maternal eNOS deficiency determines a fatty liver phenotype of the offspring in a sex dependent manner, Epigenetics : official journal of the DNA Methylation Society, 11 (2016) 539-552.

[63] C. Reichetzeder, S.E. Dwi Putra, J. Li, B. Hocher, Developmental Origins of Disease - Crisis Precipitates Change, Cell Physiol Biochem, 39 (2016) 919-938.

[64] N.C. Harvey, P.A. Mahon, S.M. Robinson, C.E. Nisbet, M.K. Javaid, S.R. Crozier, H.M. Inskip, K.M. Godfrey, N.K. Arden, E.M. Dennison, C. Cooper, S.W.S.S. Group, Different indices of fetal growth predict

bone size and volumetric density at 4 years of age, Journal of bone and mineral research : the official journal of the American Society for Bone and Mineral Research, 25 (2010) 920-927.

[65] E.M. Dennison, H.E. Syddall, A.A. Sayer, H.J. Gilbody, C. Cooper, Birth weight and weight at 1 year are independent determinants of bone mass in the seventh decade: the Hertfordshire cohort study, Pediatric research, 57 (2005) 582-586.

[66] D.A. Bailey, H.A. McKay, R.L. Mirwald, P.R. Crocker, R.A. Faulkner, A six-year longitudinal study of the relationship of physical activity to bone mineral accrual in growing children: the university of Saskatchewan bone mineral accrual study, Journal of bone and mineral research : the official journal of the American Society for Bone and Mineral Research, 14 (1999) 1672-1679.

[67] C. Cooper, J.G. Eriksson, T. Forsen, C. Osmond, J. Tuomilehto, D.J. Barker, Maternal height, childhood growth and risk of hip fracture in later life: a longitudinal study, Osteoporos Int, 12 (2001) 623-629.

[68] S.A. Lanham, C. Roberts, M.J. Perry, C. Cooper, R.O. Oreffo, Intrauterine programming of bone. Part 2: alteration of skeletal structure, Osteoporos Int, 19 (2008) 157-167.

[69] B.F. Hales, DNA repair disorders causing malformations, Curr Opin Genet Dev, 15 (2005) 234-240.

[70] J.M. Burnell, E.J. Teubner, A.G. Miller, Normal maturational changes in bone matrix, mineral, and crystal size in the rat, Calcif Tissue Int, 31 (1980) 13-19.

[71] R.M. Wilson, J.C. Elliott, S.E.P. Dowker, Rietveld refinement of the crystallographic structure of human dental enamel apatites, Am Mineral, 84 (1999) 1406-1414.

[72] J.D. Almer, S.R. Stock, Internal strains and stresses measured in cortical bone via high-energy X-ray diffraction, Journal of structural biology, 152 (2005) 14-27.

[73] R.G. Handschin, W.B. Stern, X-Ray-Diffraction Studies on the Lattice Perfection of Human Bone Apatite (Crista-Iliaca), Bone, 16 (1995) S355-S363.

Table 1. Fetal femur weight and Inductive Coupled Plasma (ICP) elemental analysis

	NPD	LPD
Right Femur weight (mg)	0.30 ± 0.02[a]	0.38 ± 0.02[b]
Right Femur calcium content (%/mg bone)	4.29 ± 0.53[a]	4.12 ± 0.21[a]
Right Femur phosphorus content (%/mg bone)	3.52 ± 0.38[a]	3.47 ± 0.14[a]
Right Femur calcium:phosphorus ratio	1.21 ± 0.03[a]	1.20 ± 0.03[a]

All data are expressed as mean ± SEM. Different superscript letters denote significance at $P < 0.05$. n = 8 femurs per dietary group, each from different litters.

Fig 1. Paternal LPD modifies preimplantation blastocyst AMPK pathway gene expression.

Fold expression change in LPD blastocysts for all array genes analysed compared with NPD genes (a). Relative LPD E3.5 blastocyst expression of genes involved in (b) metabolism, (c) receptors, (d) transcription regulation, (e) signalling cascades and (f) protein synthesis within the AMPK pathway. NPD blastocyst expression is normalised to 1; n = 4 pools of 25 blastocysts, each pool generated from 4-6 females for each dietary group. Expression data was analysed using the web-based PCR Array Data Analysis software (www.SAbiosciences.com). Bars in A represent mean with 5-95 percentile. Scatter plots display mean ± SEM. *, $P < 0.05$; **, $P < 0.01$.

Fig 2. Paternal LPD enhances late gestation fetal growth.

Mean weight of concepti, fetal and extra-embryonic tissues (a) and fetal:organ weight ratios (b) for offspring from NPD and LPD fed males at E17. Fetal liver expression of AMPK pathway genes (C); relative expression for NPD fetal livers are normalised to 1. Fetal weights are from a total of 54-59 individual fetuses from 8 litters per treatment group, each from different males. All data were analysed using a multilevel random effects regression analysis. Liver expression data are from 8 individual fetuses per treatment group, each from separate litters. Values are mean ± SEM. *, $P < 0.05$; ***, $P < 0.001$.

Fig 3. Paternal LPD modifies late gestation placental development, nutrient transporter and imprinted gene expression.

Representative mid-sagittal histological image of a late gestation placenta displaying the trophoblast (Tr), junctional (Jz) and labyrinth (Lz) zone regions (a). Total cross-sectional area of mid-sagittal sections of placental tissue and individual regions (b). Relative proportion of trophoblast, junctional zone and labyrinth zone as a percentage of the whole cross-sectional area (c). Relative LPD expression of placental transporters (d), DNA methyltransferases (e) and imprinted genes (f); expression for NPD placentas is normalised to 1. Placental morphology data are from 10 placentas

per treatment group (taken from all 8 litters per treatment group). Gene, expression analysis was conducted on 8 separate placentas per treatment group, one placenta per litter per treatment group. All data were analysed using a multilevel random effects regression analysis. Values are mean ± SEM. *, $P < 0.05$; **, $P < 0.01$.

Fig 4. Paternal diet increased late gestation fetal skeletal volume but impairs bone mineral distribution.

Representative µ-CT image of a whole E17 fetal skeleton (a). Offspring whole skeletal bone mineral density (b). Offspring whole skeletal volume (c). Litter total mineral content (d). Offspring skeletal mineral density distribution and area under the distribution curve (insert) (e). z-score transformation of offspring skeletal mineral density distribution (f). Area of offspring bone displaying low (g) or high (h) mineral density. Values in b, c, d, e, g and h are mean ± SEM. Values in F are standardised to a mean of 0 with an SD of 1. All data are from 8 fetuses per treatment group, one fetus per litter per treatment group. All data were analysed using a multilevel random effects regression analysis. *, $P < 0.05$; **, $P < 0.01$; **** P, < 0.0001.

Fig 5. Paternal LPD modifies fetal bone hydroxyapatite crystal structure

Diagram of atomic organisation and lattice plane orientation of hydroxyapatite (a). Representative X-ray diffraction pattern showing characteristic 002 and 300 rings (b). X-ray diffraction spectra (Q) averaged for NPD and LPD fetal humerus and femur hydroxyapatite (c). NPD and LPD fetal femur hydroxyapatite a=b lattice (d), a=b lattice full width half max (e), c lattice (f) and c lattice full with half max parameters (g). Values in b-d are mean ± SEM. All data are from 8 fetuses per treatment group, one fetus per litter per treatment group. All data were analysed using a multilevel random effects regression analysis. ****, $P < 0.0001$.

Fig. 1

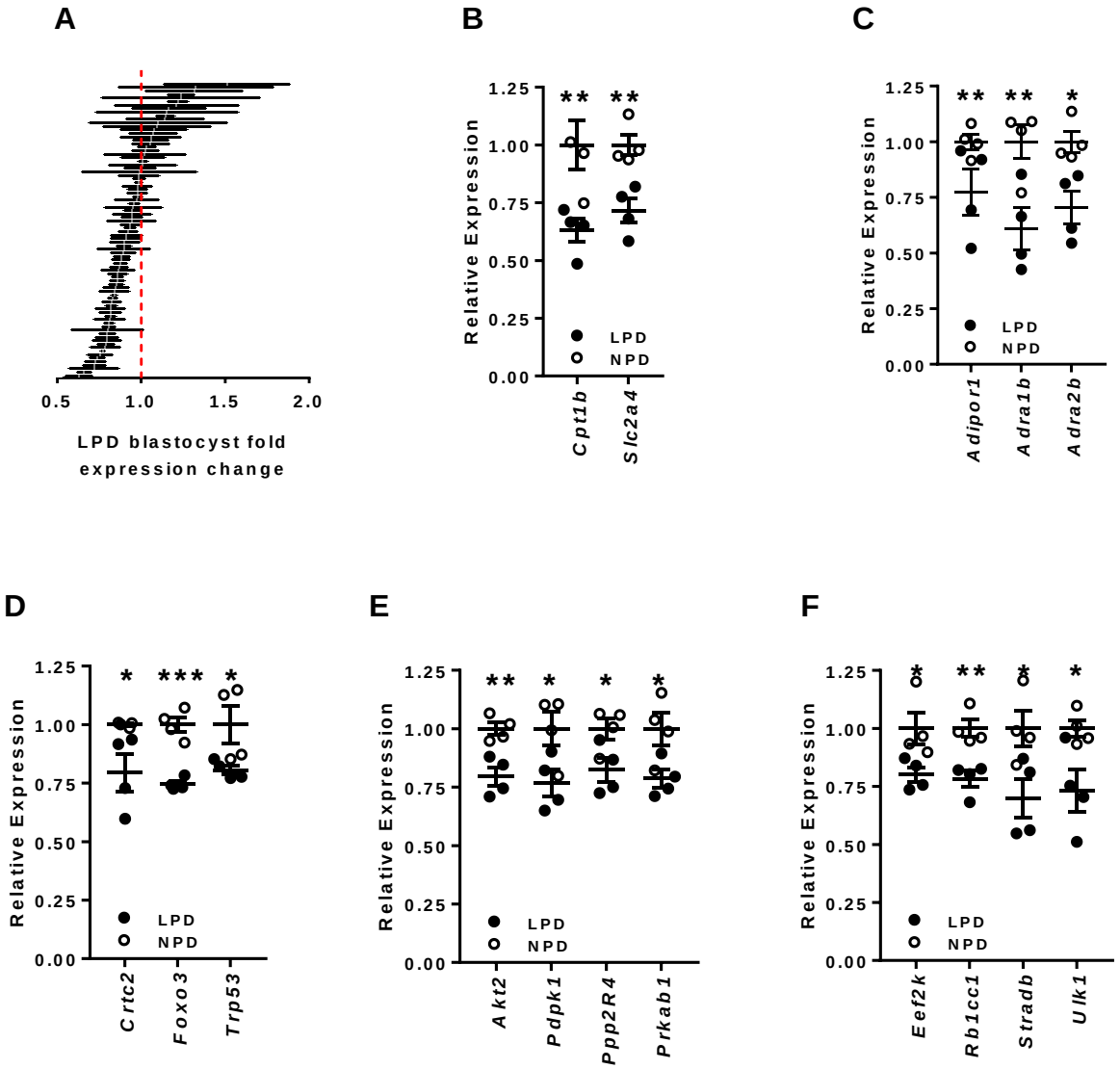
A
0.5
1.0
1.5
2.0
LPD blastocyst fold expression change
B
Relative Expression
1.25
1.00
0.75
0.50
0.25
0.00
LPD
NPD
Cpt1b
Slc2a4
C
Adipor1
Adra1b
Adra2b
D
Crtc2
Foxo3
Trp53
E
Akt2
Pdpk1
Ppp2R4
Prkab1
F
Eef2k
Rb1cc1
Stradb
Ulk1

Fig. 2

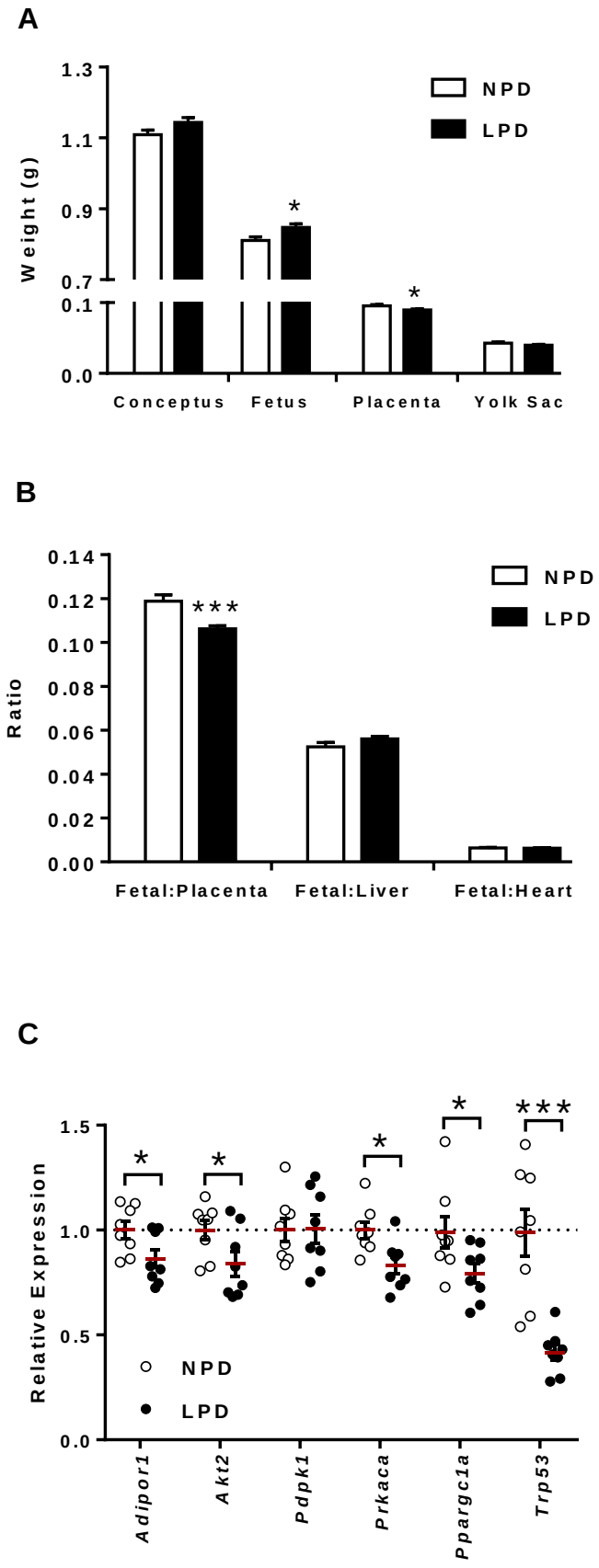
A
1.3
1.1
0.9
0.7
0.1
0.0
Weight (g)
NPD
LPD
*
*
Conceptus
Fetus
Placenta
Yolk Sac
B
0.14
0.12
0.10
0.08
0.06
0.04
0.02
0.00
Ratio
***
NPD
LPD
Fetal:Placenta
Fetal:Liver
Fetal:Heart
C
1.5
1.0
0.5
0.0
Relative Expression
*
*
*
*
***
NPD
LPD
Adipor1
Akt2
Pdpk1
Prkaca
Ppargc1a
Trp53

Fig. 3

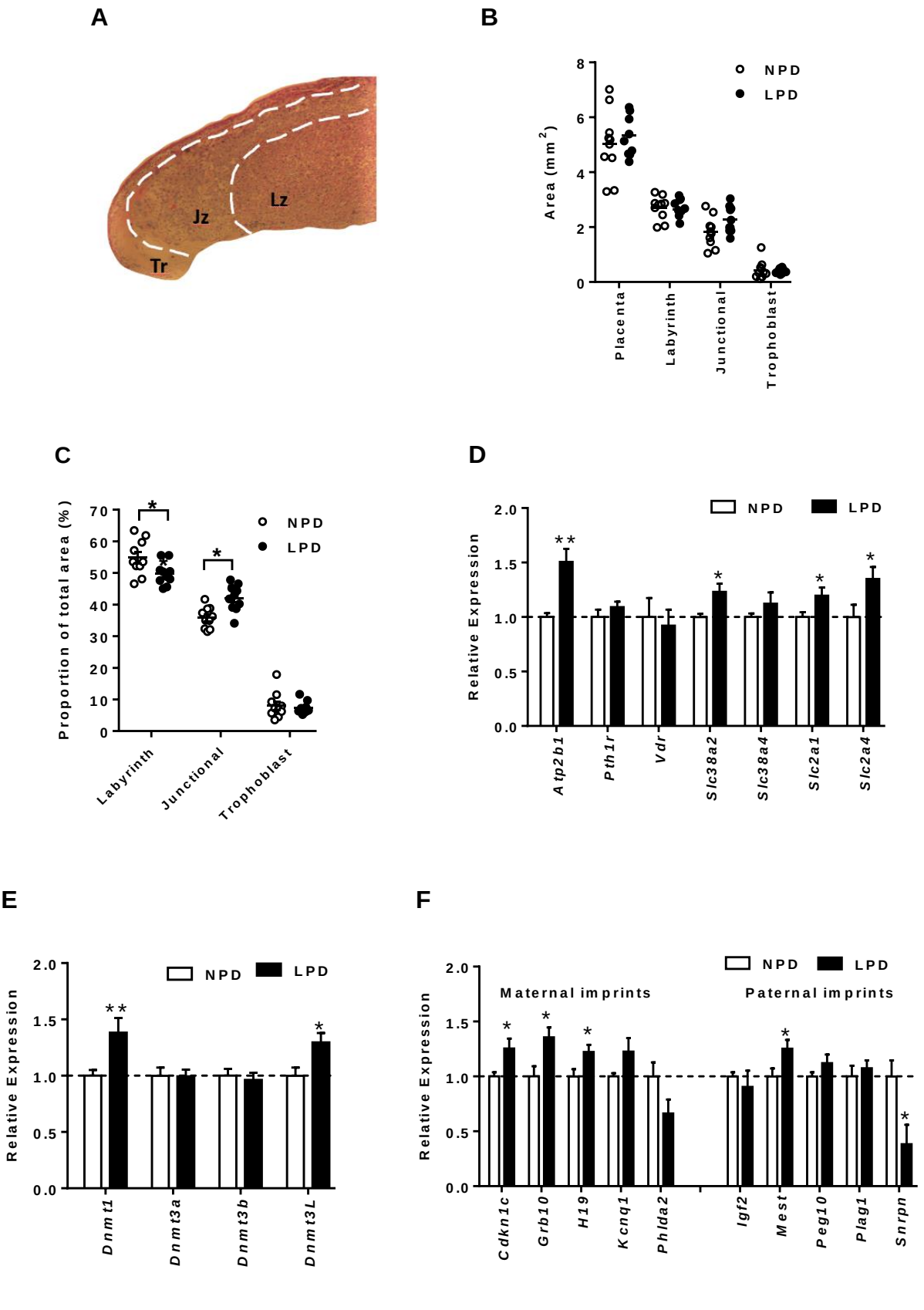
A
Jz
Lz
Tr
B
NPD
LPD
Area (mm2)
Placenta
Labyrinth
Junctional
Trophoblast
C
Proportion of total area (%)
NPD
LPD
Labyrinth
Junctional
Trophoblast
D
Relative Expression
NPD
LPD
Atp2b1
Pth1r
Vdr
Slc38a2
Slc38a4
Slc2a1
Slc2a4
E
Relative Expression
NPD
LPD
Dnmt1
Dnmt3a
Dnmt3b
Dnmt3L
F
Relative Expression
NPD
LPD
Maternal imprints
Paternal imprints
Cdkn1c
Grb10
H19
Kcnq1
Phlda2
Igf2
Mest
Peg10
Plag1
Snrpn

Fig. 4

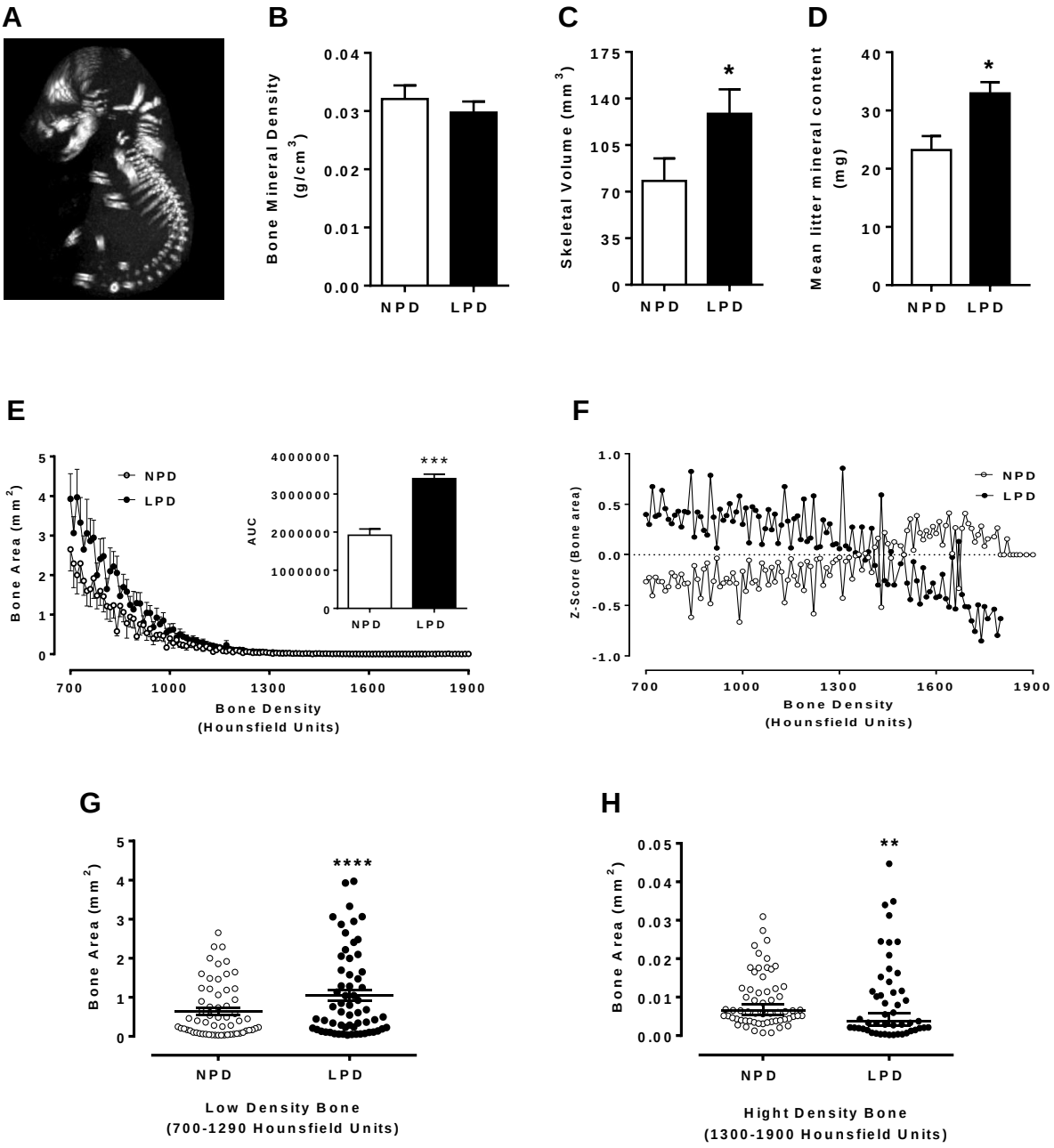
A
B
Bone Mineral Density (g/cm3)
0.04
0.03
0.02
0.01
0.00
NPD
LPD
C
Skeletal Volume (mm3)
175
140
105
70
35
0
*
NPD
LPD
D
Mean litter mineral content (mg)
40
30
20
10
0
*
NPD
LPD
E
Bone Area (mm2)
5
4
3
2
1
0
NPD
LPD
700
1000
1300
1600
1900
Bone Density
(Hounsfield Units)
AUC
4000000
3000000
2000000
1000000
0
***
NPD
LPD
F
Z-Score (Bone area)
1.0
0.5
0.0
-0.5
-1.0
NPD
LPD
700
1000
1300
1600
1900
Bone Density
(Hounsfield Units)
G
Bone Area (mm2)
5
4
3
2
1
0
****
NPD
LPD
Low Density Bone
(700-1290 Hounsfield Units)
H
Bone Area (mm2)
0.05
0.04
0.03
0.02
0.01
0.00
**
NPD
LPD
Hight Density Bone
(1300-1900 Hounsfield Units)

Fig. 5

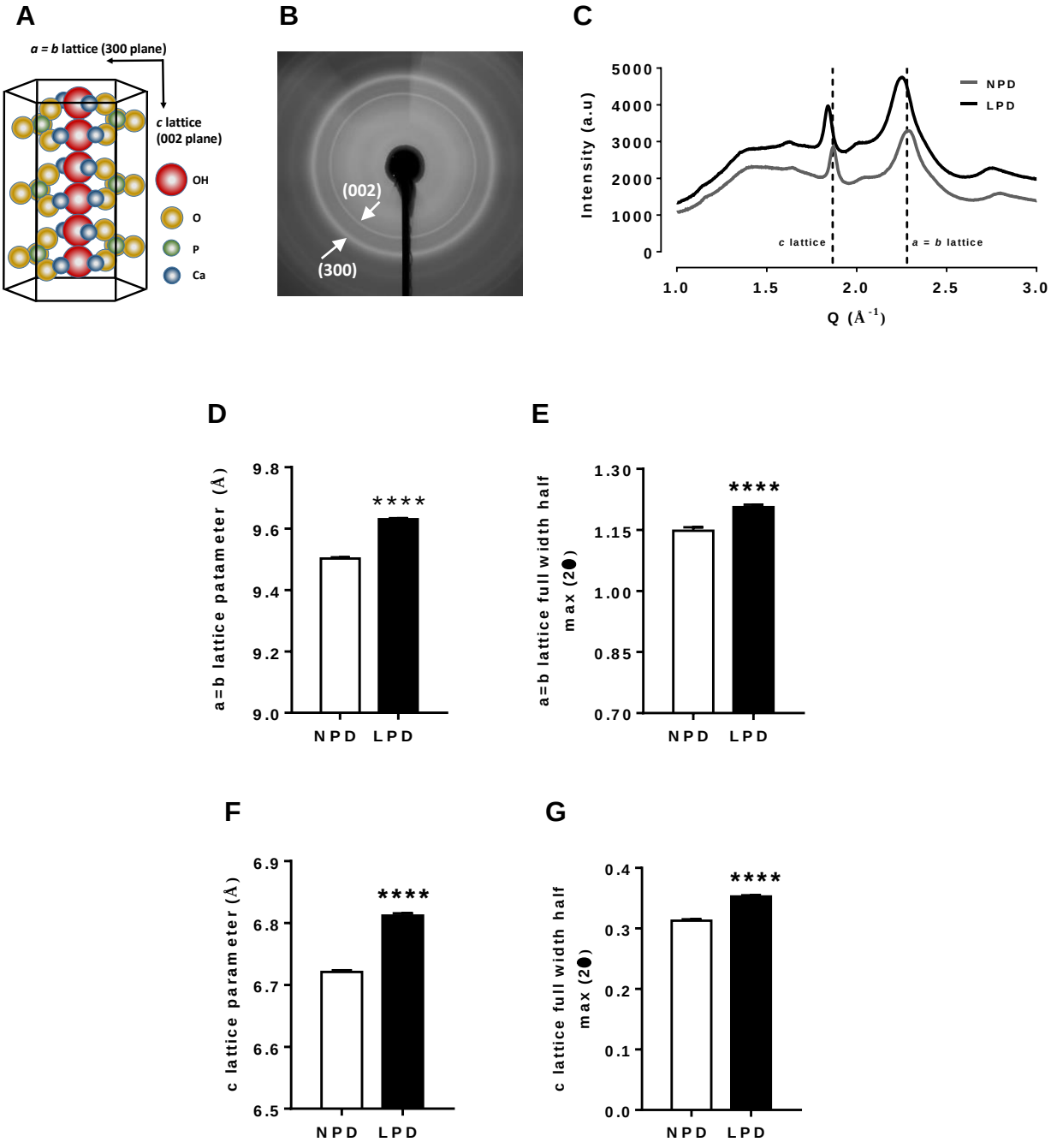
A
a = b lattice (300 plane)
c lattice
(002 plane)
OH
O
P
Ca
B
(002)
(300)
C
Intensity (a.u)
5000
4000
3000
2000
1000
0
NPD
LPD
c lattice
a = b lattice
1.0
1.5
2.0
2.5
3.0
Q (Å -1)
D
a=b lattice patameter (Å)
9.8
9.6
9.4
9.2
9.0
****
NPD
LPD
E
a=b lattice full width half max (2●)
1.30
1.15
1.00
0.85
0.70
****
NPD
LPD
F
c lattice parameter (Å)
6.9
6.8
6.7
6.6
6.5
****
NPD
LPD
G
c lattice full width half max (2●)
0.4
0.3
0.2
0.1
0.0
****
NPD
LPD